

# **The Up-Link Problem: Using RytovProp For Beam Propagation Calculations-- Conference Proceedings (Postprint)**

**David L. Fried  
14671 Tumbleweed Lane  
Watsonville, CA 95076-9259**

**01 August 2008**

**Technical Paper**

**APPROVED FOR PUBLIC RELEASE; DISTRIBUTION IS UNLIMITED.**



**AIR FORCE RESEARCH LABORATORY  
Directed Energy Directorate  
3550 Aberdeen Ave SE  
AIR FORCE MATERIEL COMMAND  
KIRTLAND AIR FORCE BASE, NM 87117-5776**

REPORT DOCUMENTATION PAGE				Form Approved OMB No. 0704-0188	
Public reporting burden for this collection of information is estimated to average 1 hour per response, including the time for reviewing instructions, searching existing data sources, gathering and maintaining the data needed, and completing and reviewing this collection of information. Send comments regarding this burden estimate or any other aspect of this collection of information, including suggestions for reducing this burden to Department of Defense, Washington Headquarters Services, Directorate for Information Operations and Reports (0704-0188), 1215 Jefferson Davis Highway, Suite 1204, Arlington, VA 22202-4302. Respondents should be aware that notwithstanding any other provision of law, no person shall be subject to any penalty for failing to comply with a collection of information if it does not display a currently valid OMB control number. <b>PLEASE DO NOT RETURN YOUR FORM TO THE ABOVE ADDRESS.</b>					
1. REPORT DATE (DD-MM-YYYY) 01-08-2008		2. REPORT TYPE Technical Paper		3. DATES COVERED (From - To) 01 Sept 06- 01 Aug 2008	
4. TITLE AND SUBTITLE The Up-Link Problem: Using RytovProp For Beam Propagation Calculations-- Conference Proceedings (Postprint)				5a. CONTRACT NUMBER FA9451-06-C-0348	
				5b. GRANT NUMBER	
				5c. PROGRAM ELEMENT NUMBER 63845F	
6. AUTHOR(S)  David L. Fried 14671 Tumbleweed Lane Watsonville, CA 95076-9259				5d. PROJECT NUMBER  52	
				5e. TASK NUMBER 99	
				5f. WORK UNIT NUMBER SVAF	
7. PERFORMING ORGANIZATION NAME(S) AND ADDRESS(ES) David L. Fried Address City, State Zip				8. PERFORMING ORGANIZATION REPORT NUMBER	
9. SPONSORING / MONITORING AGENCY NAME(S) AND ADDRESS(ES)  Air Force Research Laboratory 3550 Aberdeen Ave SE Kirtland AFB NM 87117-5776				10. SPONSOR/MONITOR'S ACRONYM(S) AFRL/RDSA	
				11. SPONSOR/MONITOR'S REPORT NUMBER(S) AFRL-RD-PS-TP-2008-1010	
12. DISTRIBUTION / AVAILABILITY STATEMENT  Approved for Public Release; Distribution is Unlimited.					
13. SUPPLEMENTARY NOTES Published in 2008 AMOS Conference, Sept. 15-19, 2008, Fried. "Government Purpose Rights"					
14. ABSTRACT RytovProp is a new approach to the task of generating a large number of random realizations manifesting some aspect(s) of the effect of turbulence on optical propagation. This method has been applied to the evaluation of Up-Link performance—delivery of laser power from a simple ground transmitter to a satellite. This computational method allows the development of hundreds of thousands of statistically independent random realizations of the laser power density at the satellite in just one or two minutes on an ordinary PC.					
15. SUBJECT TERMS					
16. SECURITY CLASSIFICATION OF:			17. LIMITATION OF ABSTRACT  SAR	18. NUMBER OF PAGES  27	19a. NAME OF RESPONSIBLE PERSON Earl Spillar
a. REPORT Unclassified	b. ABSTRACT Unclassified	c. THIS PAGE Unclassified			19b. TELEPHONE NUMBER (include area code) 505- 846-6740

Standard Form 298 (Rev. 8-98)  
Prescribed by ANSI Std. Z39.18

**The Up-Link Problem:  
Using RytovProp For  
Beam Propagation Calculations**

David L. Fried

August 2008

## ABSTRACT

RytovProp is a new approach to the task of generating a large number of random realizations manifesting some aspect(s) of the effect of turbulence on optical propagation. This method has been applied to the evaluation of Up-Link performance—delivery of laser power from a simple ground transmitter to a satellite. This computational method allows the development of hundreds of thousands of statistically independent random realizations of the laser power density at the satellite in just one or two minutes on an ordinary PC.

The RytovProp method is based on use of

- analytic results for the phase structure function, the log-amplitude covariance, and the phase:log-amplitude cross-covariance, that have been developed using the Rytov approximation,
- the assumption that turbulence induced phase and log-amplitude perturbations are jointly gaussian random variables, and
- a “little trick” from statistics/matrix-theory that allows a realization of a set of random variables to be very easily/quickly developed given the covariance matrix relating all of the random variables with each other.

The “little trick” is the following. Given a covariance matrix, and using the fact that for any covariance matrix it is possible to generate a real matrix which when multiplied by its transpose will be equal to the covariance matrix—a matrix which may be considered to be the square root of the covariance matrix, then it can be shown that this square root matrix when it multiplies a column vector of normally distributed, statistically independent random values will produce a column vector of gaussian random values for which the covariance between any pair of elements of this column vector will be equal to the corresponding element of the original covariance matrix.

This means that if the covariance matrix is one relating the turbulence perturbed phases and log-amplitudes of the contributions to the optical field at the satellite from each of an array of points covering the transmitter aperture, then these elements of the product column vector (plus any applicable mean values) can be taken as suitably chosen random realizations of these turbulence perturbed phases and log-amplitudes of the contributions to the optical field at the satellite from each of an array of points covering the transmitter aperture. From these random phase and log-amplitude values the laser power density at the satellite can be calculated.

With suitable modifications this computational method can be made to incorporate the effect of rapid tip/tilt adjustment of the transmitted laser beam—these adjustments being based on tracking of the satellite. Such modifications of the method can be made to incorporate the effects of both anisoplanatism and of finite tip/tilt tracking servo bandwidth.

In this paper the relevant theory is presented along with sample numerical results comparing probability distributions developed using the RytovProp method and using the (orders of magnitude slower) split-step wave optics propagation method—the comparisons generally showing good agreement.

## 1. Introduction

I use the term “Up-Link” to refer to a ground-to-space optical communications system—a system that establishes a link from a ground based laser transmitter to a receiver on an orbiting satellite. I take as the “Up-Link Problem” the task of developing statistical results characterizing the effects of atmospheric turbulence on the signal strength of such a link—in particular the task of developing results for the signal strength’s probability distribution.

The Up-Link Problem is a subject that has been of interest for many years. Most of the prior work has been devoted to attempts to develop analytic formulations—with only limited success. Because of analytic difficulties/limitations when quantitative results were required a great deal of reliance had to be placed on a Monte Carlo based approach with each random realization of the signal strength being developed using wave optics propagation simulation computations.

In preparation for such wave optics propagation computations

- the propagation path is divided into a (presumably large) number,  $N$ , of segments—with the locations along the propagation path of  $N$  associated mid-segment planes being defined (along with an aperture-plane located at the ground end of the propagation path and a receiver-plane located at the satellite end of the propagation path, for a total of  $N + 2$  planes),
- a two-dimensional grid pattern count-size (for example 1024-by-1024) is selected,

and

- a set of physical length that are to be associated with the two sides of each of the  $N + 2$  grid patterns is defined.

Also in preparation for wave optics propagation simulation computations

- a scalar-field representation of the laser beam as it would leave the aperture of the ground based transmitter system (as it would leave—but before any transmitter adaptive optics or tilt correction is applied) is defined.

The Monte Carlo method relies on wave optics propagation simulation computations to generate a large number,  $K$ , of random realizations of the scalar optical field at the receiver-plane, calculates the signal strength that is to be associated with this scalar field for each of the  $K$  realizations, and then forms an estimate of the statistical parameters that characterize the random variations of the signal strength from these  $K$  different realizations of the signal strength. If  $K$  is large enough and if there is sufficient statistical independence amongst these  $K$  realizations of the strength of the signal, then the estimates of these statistical parameters will be sufficiently accurate.

Regarding the statistical independence of this collection of  $K$  results for the signal strength the following should be noted.

- The wave optics propagation calculations are carried out with a set of  $N$  randomly chosen turbulence pattern realizations, one for each of the  $N$  mid-segment planes—each of these  $N$  patterns being chosen in a way that is statistically compatible with the expected optical strength of turbulence in the corresponding one of the  $N$  segments of the propagation path.
- In most cases it is necessary to run the simulation over a sequence of instants of time—shifting the random turbulence patterns from instant-to-instant in a manner that represents the effect of line-of-sight slewing (associated with tracking the moving satellite) and the effect of the ambient winds—to properly initialize the operation of the adaptive optics and/or the tilt tracking systems.

- While wave optics propagation calculations may be conducted in such a way that for each of the  $K$  results for the signal strength a set of  $N$  turbulence patterns unique to that value of the signal strength will have been chosen, in general the instant-to-instant sequence of operation is continued for a long sequence of instants (after initialization is completed) and for each instant (except the first few which are required for initialization) a signal strength value is developed—all of which signal strength values go into making up the set of  $K$  signal strength values used in forming the estimated values of the statistical parameters. This has the negative effect that

- successive values of the signal strength are strongly correlated, accordingly reducing the number of degrees-of-freedom in the set of  $K$  signal strength values

from which it follows that

- the accuracy of the estimates of the statistical parameters describing the random variations of the signal strength is reduced.

That a long sequence of instants, with associated signal strength values, computed with the same (continuously shifted) set of  $N$  turbulence patterns, is used to provide multiple contributions to the set of  $K$  signal strength values—that it is used despite the consequent reduction in the number of degrees-of-freedom in the set of  $K$  signal strength values and degradation of the accuracy of the estimated statistical parameters—reflects the general slowness of the wave optics propagation computational method. To generate  $K$  statistically independent values for the signal strength would require considerably more time, and this is generally not done because of the relatively large amount of time it takes to develop wave optics propagation results for each instant.

The RytovProp method, the presentation of which is the subject of this paper, has been designed to produce a large set of statistically independent random results for the signal strength, and to be able to carry this out very rapidly (*i.e.* orders of magnitude more rapidly than can be done using a wave optics propagation based approach), thus supporting a Monte Carlo based approach to the Up-Link Problem. It is to be noted that, in distinction to wave optics propagation simulation, the soundness of the analytic basis for the RytovProp method is limited to the propagation regime for which the value of the Rytov number (*i.e.* the value of the log-amplitude variance computed using the Rytov approximation) is significantly less than unity.

## 2. Calculating The Signal Strength At The Receiver Plane

For RytovProp calculations I consider a square patterned lattice of points on the aperture plane of the ground based laser transmitter, an array of points sufficiently dense that it can be considered to adequately sample the aperture. I chose the spacing between adjacent lattice points to be such that there are  $P$  lattice points within the aperture, denoting their positions by  $\mathbf{r}_p = (x_p, y_p)$  where  $p = \{1, 2, 3, \dots, P\}$ . I shall use the notation  $\mathbf{r}_0$  to denote the center of the aperture and will adjust/shift the placement of this lattice of points so that it is symmetric about this center-point but does not include that center-point—so the center-point (at  $\mathbf{r}_0$ ) will be in the center of the small square formed by the four points of the lattice that are closest to  $\mathbf{r}_0$ . There are thus  $P + 1$  points/positions defined on the aperture of the laser transmitter.

I use the notation  $t_0$  to denote what I call the “current time on the ground.” By this phrase I mean the time to be associated with a value of the signal strength at the receiver at some instant, but I take this time as being that of the instant, at the ground, when that signal was transmitted. (Thus when I speak of a time,  $t_0$ , this time is to be associated with the signal at the receiver on the satellite

but it is to be understood that what is being referred to is the time when that received signal left the ground based transmitter.) There is of course some time required for light to propagate from the ground to the satellite—so the time when the signal actually is received at the satellite is latter than  $t_0$ , but that latter time *per se* plays no part in the analysis that I am presenting here. Associated with the current time,  $t_0$ , I will use the notation  $\theta_0$  to denote the direction in which the laser signal is transmitted at time  $t_0$ .

I shall consider a sequence of  $M$  prior times,  $t_m$ , where  $m = \{1, 2, 3, \dots, M\}$ —times when beacon-signals, originating from the satellite, are received on the ground—received from the corresponding sequence of direction,  $\theta_m$ . It is to be noted that these directions vary linearly with the time. To extend this understanding regarding the direction notation so that it will also apply to the current time,  $t_0$ , and its associated direction,  $\theta_0$ , it is to be noted that in its relation to all the other directions,  $\theta_m$ , the value of  $\theta_0$  follows this same linear variation with time *except* for the presence of an additive constant, a constant that is equal to the so called point-ahead angle. For the current time,  $t_0$ , I am interested in transmission of the laser beam to the satellite rather than in reception of the beacon from the satellite, so the corresponding (transmission) direction,  $\theta_0$ , must be off-set from the direction in which a beacon would be received from the satellite at that time by the point-ahead angle—the angle that a transmitted laser beam nominally has to lead the apparent direction to the satellite if the laser beam is to be incident on the satellite.

The RytovProp method considers optical propagation between each of the  $P + 1$  points,  $\mathbf{r}_p$ , where  $p = \{0, 1, 2, 3, \dots, P\}$  on the plane of the laser transmitter aperture and a receiver/beacon point on the satellite—which receiver/beacon point, because of the satellite's motion, has a position that depends on time, being different for each of the  $M + 1$  times in the set consisting of the current time,  $t_0$ , and the  $M$  prior times,  $t_m$  where  $m = \{1, 2, 3, \dots, M\}$ —*i.e.* the set  $t_m$  with  $m = \{0, 1, 2, 3, \dots, M\}$ . I use the notation  $\phi_{p,m}$  and  $\ell_{p,m}$  to denote the turbulence induced perturbation of the phase and of the log of the amplitude respectively of the optical field in propagation between the point at  $\mathbf{r}_p$  on the plane of the transmitter aperture and the location of the receiver/beacon point on the satellite at time  $t_m$ . It is to be noted that, by virtue of the reciprocity principle in optical propagation between two points, it is not necessary to indicate which is the source point; the same values for the phase and log-amplitude perturbations apply which ever one of the two points is the source point.

If a statistically appropriate randomly selected realization of the set of  $P \times (M + 1)$  values for the turbulence induced phase perturbations,  $\phi_{p,m}$ , and for the set of  $P$  values for the turbulence induced log-amplitude perturbations,  $\ell_{p,0}$ , were available then the Strehl ratio associated with the signal strength,  $\mathcal{S}$ , could be calculated according to the formula that

$$\mathcal{S} = \frac{\left| \sum_{p=1}^P A_p \Delta^2 \exp \left( \ell_{p,0} + i [\phi_{p,0} - \varphi_p] \right) \right|^2}{\left| \sum_{p=1}^P A_p \Delta^2 \right|^2}, \quad (1)$$

where  $A_p$  represents the amplitude of the laser beam at position  $\mathbf{r}_p$  on the transmitter's aperture,  $\Delta$  represents the distance between adjacent points in the set of  $P$  points covering the transmitter's aperture, and  $\varphi_p$  represents phase shift at position  $\mathbf{r}_p$  on the transmitter's aperture that is to be associated with the adaptive optics and/or tilt corrections.

The value of  $\varphi_p$  may be considered to be formed as a weighted sum of all of the  $m = \{1, 2, 3, \dots, M\}$  prior time phase values,  $\phi_{p,m}$ , at all of the  $p = \{1, 2, 3, \dots, P\}$  positions on the aperture. The  $m$ -dependence of the values of the weighting factors (along with the values,  $t_m$ , of the prior times) defines the servo bandwidth of the adaptive optics and/or tilt tracking control systems.

For the Up-Link Problem I restrict attention to transmitter systems with only tilt tracking controls. For such a system, using the notation  $k$  to denote the optical wave number, where

$$k = 2\pi/\lambda, \quad (2)$$

with  $\lambda$  denoting the laser (and beacon) wave length, the value of  $\varphi_p$  may be considered to be given by the equation

$$\varphi_p = k (\tilde{x}_p \vartheta^x + \tilde{y}_p \vartheta^y), \quad (3)$$

where

$$\tilde{x}_p = \frac{x_p - \bar{x}}{\sqrt{\sum_{p'=1}^P (x_{p'} - \bar{x})^2}}, \quad \text{and} \quad \tilde{y}_p = \frac{y_p - \bar{y}}{\sqrt{\sum_{p'=1}^P (y_{p'} - \bar{y})^2}}, \quad (4)$$

with

$$\bar{x} = \sum_{p=1}^P x_p, \quad \text{and} \quad \bar{y} = \sum_{p=1}^P y_p, \quad (5)$$

so that

$$\sum_{p=1}^P \tilde{x}_p = 0, \quad \text{and} \quad \sum_{p=1}^P \tilde{y}_p = 0, \quad (6)$$

and

$$\sum_{p=1}^P \tilde{x}_p^2 = 1, \quad \text{and} \quad \sum_{p=1}^P \tilde{y}_p^2 = 1, \quad (7)$$

and where

$$\vartheta^x = \sum_{m=1}^M \alpha_m \vartheta_m^x, \quad \text{and} \quad \vartheta^y = \sum_{m=1}^M \alpha_m \vartheta_m^y, \quad (8)$$

with the set of  $M$  different values of  $\alpha_m$  representing the above mentioned weighting factors—a set of coefficients that may be thought of as defining the bandwidth of the beacon-tip/tilt tracking servo system. The quantities  $\vartheta_m^x$  and  $\vartheta_m^y$  represent the two components of the beacon tilt,  $\boldsymbol{\vartheta}_m$ , measured at the  $m^{\text{TH}}$  prior time,  $t_m$ , and may be considered to have values given by the equation

$$\vartheta_m^x = k^{-1} \sum_{p=1}^P \tilde{x}_p \phi_{p,m}, \quad \text{and} \quad \vartheta_m^y = k^{-1} \sum_{p=1}^P \tilde{y}_p \phi_{p,m}. \quad (9)$$

At this point it is appropriate to note that by virtue of Eq. (6) I can recast Eq. (9) as

$$\begin{aligned} \vartheta_m^x &= k^{-1} \sum_{p=1}^P \tilde{x}_p \{ \phi_{p,m} - \phi_{0,m} \} & \text{and} & & \vartheta_m^y &= k^{-1} \sum_{p=1}^P \tilde{y}_p \{ \phi_{p,m} - \phi_{0,m} \} \\ &= k^{-1} \sum_{p=1}^P \tilde{x}_p \tilde{\phi}_{p,m}, & & & &= k^{-1} \sum_{p=1}^P \tilde{y}_p \tilde{\phi}_{p,m}, \end{aligned} \quad (10)$$

where

$$\tilde{\phi}_{p,m} = \phi_{p,m} - \phi_{0,m}. \quad (11)$$

I will refer to the quantity denoted by  $\tilde{\phi}_{p,m}$  as the “adjusted phase perturbation.”



It is also to be noted here that since  $|\exp(i\phi_{0,m})|^2 = 1$  then Eq. (1) can be rewritten as

$$\begin{aligned} \mathcal{S} &= \frac{\left| \sum_{p=1}^P A_p \Delta^2 \exp \left( [\{\ell_{p,0} - \bar{\ell}\} + \bar{\ell}] + i[\{\phi_{p,0} - \phi_{0,0}\} - \varphi_p] \right) \right|^2}{\left| \sum_{p=1}^P A_p \Delta^2 \right|^2} \\ &= \frac{\left| \sum_{p=1}^P A_p \exp \left( [\tilde{\ell}_{p,0} + \bar{\ell}] + i[\tilde{\phi}_{p,0} - \varphi_p] \right) \right|^2}{\left| \sum_{p=1}^P A_p \right|^2}, \end{aligned} \quad (12)$$

where

$$\tilde{\ell}_{p,m} = \ell_{p,m} - \bar{\ell}, \quad (13)$$

with  $\bar{\ell}$  denoting the mean (*i.e.* the ensemble average) value of the turbulence induced log-amplitude perturbations, which mean value is independent of the position,  $\mathbf{r}_p$ , and of the time,  $t_m$ , and is defined by the equation

$$\bar{\ell} = \langle \ell_{p,m} \rangle. \quad (14)$$

I will refer to the quantity denoted by  $\tilde{\ell}_{p,m}$  as the “adjusted log-amplitude perturbation,” and will refer to the quantity denoted by  $\bar{\ell}$  as the “log-amplitude expected value.”

It can be seen that given a set of statistically appropriate randomly selected<sup>1</sup> value for  $\tilde{\phi}_{p,m}$  for all  $p = \{1, 2, 3, \dots, P\}$  and all  $m = \{0, 1, 2, 3, \dots, M\}$ —a total of  $P \times (M+1)$  random values—and for  $\ell_{p,0}$  for all  $p = \{1, 2, 3, \dots, P\}$ —a total of an additional  $P$  random values, then

- first, making use of Eq.’s (4) and (9), correspondingly statistically appropriate random pairs of value can be developed for each of the prior time tilts,  $\vartheta_m^x$  and  $\vartheta_m^y$ ,
- next, making use of Eq. (8), a correspondingly statistically appropriate pair of values can be developed for the time weighted average (servo correction) tilts,  $\vartheta^x$  and  $\vartheta^y$ ,
- following which, making use of Eq.’s (3) and (4), the set of tilt-tracking servo correction induced phase adjustments,  $\varphi_p$ , for each of the  $P$  positions,  $\mathbf{r}_p$ , can be calculated,

Using Eq. (12) I can then calculate the value of the associated (and statistically appropriate) Strehl ratio,  $\mathcal{S}$ .

This would seem to require the initial generation of a total of  $P \times (M+1) + P = P \times (M+2)$  random values for each Strehl ratio value that is produced. As will be developed latter we can “short circuit” some of this process and directly generate a set of random values for  $\tilde{\phi}_{p,0}$ ,  $\tilde{\ell}_{p,0}$  for  $p = \{1, 2, 3, \dots, P\}$ , along with random values for  $\vartheta_m^x$  and  $\vartheta_m^y$  for  $m = \{1, 2, 3, \dots, M\}$ , a

---

<sup>1</sup> By the term “statistically appropriate randomly selected” I imply that the method used for choosing values for  $\tilde{\phi}_{p,m}$  and for  $\tilde{\ell}_{p,0}$  results in values whose statistics are in accordance with all that we know of the statistics for these random variables. As will be developed latter, what we consider that we know of the statistics is 1) that these random variables, taken together, have a jointly gaussian distribution, 2) that they each have a mean value of zero, 3) what the value of the covariance of  $\tilde{\phi}_{p,m}$  with  $\tilde{\phi}_{p',m'}$  is, 4) what the value of the covariance of  $\tilde{\ell}_{p,0}$  with  $\tilde{\ell}_{p',0}$  is, and what the cross-covariance between  $\tilde{\phi}_{p,m}$  and  $\tilde{\ell}_{p',0}$  is.

set for which the combination of random values will all be statistically appropriate—a set of only  $P + P + M + M = 2(P + M)$  random values—from which a corresponding, statistically appropriate, Strehl ratio value can be developed. This can be done directly, *i.e.* without having to first generate the much larger set of randomly selected values of  $\phi_{p,m}$  for all combinations of  $p = \{1, 2, 3, \dots, P\}$  and  $m = \{1, 2, 3, \dots, M\}$ . But this will be covered in Section 4. For now I concern myself with setting forth the method of generating the full set of value of  $\tilde{\phi}_{p,m}$  along with the set of values of  $\tilde{\ell}_{p,0}$  for all values of  $p$  and  $m$ . I take this up in the next section.

### 3. Generating A Full Set Of Randomly Selected Statistically Appropriate Phase And Log-Amplitude Perturbation Values

I separate this section into three sub sections. In the first sub section I present the basic covariance matrix based approach to the generation of a set of statistically appropriate randomly selected values for a set of zero mean, gaussian random variables—providing that each of these random variables has a finite variance.

In the second sub section I present the Rytov approximation based second moment results for turbulence induced phase and log-amplitude perturbations,  $\phi_{p,m}$  and  $\ell_{p,m}$ —the second moment results referred to as the log-amplitude covariance, the phase structure function, and the phase:log-amplitude cross-covariance function.

In the third sub section I show how the second moment results for the turbulence induced phase and log-amplitude perturbations,  $\phi_{p,m}$  and  $\ell_{p,m}$ , that are presented in the second sub section may be used to develop the covariance and cross-covariance values for the adjusted phase and adjusted log-amplitude perturbations,  $\tilde{\phi}_{p,m}$  and  $\tilde{\ell}_{p,m}$ . (It is to be noted that these covariance and cross-covariance values constitute the elements of a covariance matrix that could be used—in the way set forth in the first sub section—in the generation of a statistically appropriate realization of a set of random values for the adjusted phase and adjusted log-amplitude perturbations,  $\tilde{\phi}_{p,m}$  and  $\tilde{\ell}_{p,m}$ .)

#### 3.1. Generating A Set Of Statistically Appropriate Zero-Mean, Jointly-Gaussian, Random Variables

Let  $z_n$  denote a set of  $n = \{1, 2, 3, \dots, N\}$  zero-mean, jointly-gaussian, random variables, and let  $\mathbf{z}$  denote a column vector whose  $n^{\text{TH}}$  element is  $z_n$ . Using the angle-bracket notation,  $\langle \dots \rangle$ , to indicate an ensemble average the covariance matrix,  $\mathbf{C}_z$ , for this set of random variables can be seen to be given by the equation

$$\mathbf{C}_z = \langle \mathbf{z} \mathbf{z}^T \rangle. \quad (15)$$

This is an  $N$ -by- $N$  size matrix.

Let  $\mathbf{U}_z$  denote a matrix whose columns correspond to the eigen-vectors of  $\mathbf{C}_z$ , and let  $\mathbf{S}_z$  denote a diagonal matrix whose diagonal elements are the corresponding eigen-values of  $\mathbf{C}_z$ . Both  $\mathbf{U}_z$  and  $\mathbf{S}_z$  are, like  $\mathbf{C}_z$ ,  $N$ -by- $N$  size matrices. I can write

$$\mathbf{C}_z \mathbf{U}_z = \mathbf{U}_z \mathbf{S}_z. \quad (16)$$

Because the eigen vectors are ortho-normal  $\mathbf{U}_z$  is unitary/orthogonal and I can write

$$\mathbf{U}_z^T \mathbf{U}_z = \mathbf{I}, \quad \text{as well as} \quad \mathbf{U}_z \mathbf{U}_z^T = \mathbf{I}, \quad (17)$$

where  $\mathbf{I}$  is the identity matrix of size  $N$ -by- $N$  —a diagonal matrix all of whose diagonal elements are equal to unity.

Let  $\tilde{\mathbf{S}}_z$  denote a diagonal matrix whose diagonal elements are each equal to the square root of the corresponding one of the diagonal elements of  $\mathbf{S}_z$ , so that

$$\tilde{\mathbf{S}}_z \tilde{\mathbf{S}}_z^T = \mathbf{S}_z. \quad (18)$$

Now form the matrix  $\tilde{\mathbf{C}}_z$  according to the equation

$$\tilde{\mathbf{C}}_z = \mathbf{U}_z \tilde{\mathbf{S}}_z. \quad (19)$$

It is easy to shown that this matrix,  $\tilde{\mathbf{C}}_z$ , is the square root of the matrix  $\mathbf{C}_z$  —the square root of  $\mathbf{C}_z$  in the sense that  $\tilde{\mathbf{C}}_z \tilde{\mathbf{C}}_z^T = \mathbf{C}_z$ . To prove this—successively making use of Eq. (19), (18), and (17)—I write

$$\tilde{\mathbf{C}}_z \tilde{\mathbf{C}}_z^T = (\mathbf{U}_z \tilde{\mathbf{S}}_z) (\mathbf{U}_z \tilde{\mathbf{S}}_z)^T = \mathbf{U}_z \tilde{\mathbf{S}}_z \tilde{\mathbf{S}}_z^T \mathbf{U}_z^T = \mathbf{U}_z \mathbf{S}_z \mathbf{U}_z^T = \mathbf{C}_z \mathbf{U}_z \mathbf{U}_z^T = \mathbf{C}_z. \quad (20)$$

Let  $\boldsymbol{\gamma}$  be a column vector of length  $N$  of zero-mean, unity-variance, statistically-independent, gaussian random variables, so that

$$\langle \boldsymbol{\gamma} \rangle = \mathbf{0}, \quad \text{and} \quad \langle \boldsymbol{\gamma} \boldsymbol{\gamma}^T \rangle = \mathbf{I}, \quad (21)$$

where  $\mathbf{0}$  is a column vector of length  $N$  all of whose elements are equal to zero, and as above  $\mathbf{I}$  is the identity matrix of size  $N$ -by- $N$ .

I assert that the column vector  $\boldsymbol{\zeta}$  formed according to the equation

$$\boldsymbol{\zeta} = \tilde{\mathbf{C}}_z \boldsymbol{\gamma}, \quad (22)$$

is a statistically appropriate realization of the random variable  $\mathbf{z}$ . To prove that this is so I first note that since the elements of  $\boldsymbol{\gamma}$  taken as a set of random variables constitute a realizations of a jointly gaussian set or random variables, and since the elements of  $\boldsymbol{\zeta}$  are formed as variously weighted sums of the elements of  $\boldsymbol{\gamma}$ , then the elements of  $\boldsymbol{\zeta}$  constitute a realization of a set of jointly gaussian random variables. I next note that since  $\langle \boldsymbol{\gamma} \rangle = \mathbf{0}$ , then since  $\tilde{\mathbf{C}}_z$  is non random then

$$\langle \boldsymbol{\zeta} \rangle = \langle \tilde{\mathbf{C}}_z \boldsymbol{\gamma} \rangle = \tilde{\mathbf{C}}_z \langle \boldsymbol{\gamma} \rangle = \tilde{\mathbf{C}}_z \mathbf{0} = \mathbf{0}. \quad (23)$$

Finally, I note that

$$\langle \boldsymbol{\zeta} \boldsymbol{\zeta}^T \rangle = \langle (\tilde{\mathbf{C}}_z \boldsymbol{\gamma}) (\tilde{\mathbf{C}}_z \boldsymbol{\gamma})^T \rangle = \langle \tilde{\mathbf{C}}_z \boldsymbol{\gamma} \boldsymbol{\gamma}^T \tilde{\mathbf{C}}_z^T \rangle = \tilde{\mathbf{C}}_z \langle \boldsymbol{\gamma} \boldsymbol{\gamma}^T \rangle \tilde{\mathbf{C}}_z^T = \tilde{\mathbf{C}}_z \mathbf{I} \tilde{\mathbf{C}}_z^T = \tilde{\mathbf{C}}_z \tilde{\mathbf{C}}_z^T = \mathbf{C}_z. \quad (24)$$

These three just noted fact indicate that the values of the elements of  $\boldsymbol{\zeta}$ , calculated in accordance with Eq. (22), are a statistically appropriate realization of the random variable elements of the column vector  $\mathbf{z}$ . They have the correct mean value, the correct set of covariances and cross-covariances, and are jointly gaussian.

### 3.2. Rytov Approximation Based Statistics For Turbulence Induced Phase And Log-Amplitude Perturbations

To develop values for the elements of the covariance matrix  $\mathbf{C}_z$  when the elements of  $\mathbf{z}$  correspond to the various adjusted phase and adjusted log-amplitude values,  $\tilde{\phi}_{p,m}$  and  $\tilde{\ell}_{p,m}$ , that will have to be available to allow generation of Strehl ratio values utilizing to Eq. (12), I start by defining the log-amplitude covariance function,  $\mathcal{C}_{\ell\ell}$ , the phase structure function,  $\mathcal{D}_{\phi\phi}$ , and the phase:log-amplitude cross-covariance,  $\mathcal{C}_{\phi\ell}$ , for the various combinations of aperture plane position,  $\mathbf{r}_p$  and  $\mathbf{r}_{p'}$ , and various combinations of times,  $t_m$  and  $t_{m'}$  and associated propagation directions,  $\boldsymbol{\theta}_m$  and  $\boldsymbol{\theta}_{m'}$ . These three statistical second moment quantities are defined by the equations

$$\mathcal{C}_{\ell\ell}(p, m; p', m') = \left\langle [\ell_{p,m} - \bar{\ell}] [\ell_{p',m'} - \bar{\ell}] \right\rangle, \quad (25a)$$

$$\mathcal{D}_{\phi\phi}(p, m; p', m') = \left\langle [\phi_{p,m} - \phi_{p',m'}]^2 \right\rangle, \quad (25b)$$

$$\mathcal{C}_{\phi\ell}(p, m; p', m') = \left\langle \phi_{p,m} [\ell_{p',m'} - \bar{\ell}] \right\rangle. \quad (25c)$$

It is to be noted that these quantities,  $\mathcal{C}_{\ell\ell}(p, m; p', m')$ ,  $\mathcal{D}_{\phi\phi}(p, m; p', m')$ , and  $\mathcal{C}_{\phi\ell}(p, m; p', m')$ , are defined in terms of the turbulence induced phase and log-amplitude perturbations,  $\phi_{p,m}$  and  $\ell_{p,m}$ , and not in terms of the *adjusted* phase and *adjusted* log-amplitude perturbations,  $\tilde{\phi}_{p,m}$  and  $\tilde{\ell}_{p,m}$ .

Making use of the Rytov approximation in developing a solution for the wave propagation equation, assuming that the atmospheric turbulence pattern is in accordance with the Kolmogorov theory of turbulence in the inertial sub range, and farther assuming that the time dependence of the turbulence pattern is governed by the Taylor theory of frozen turbulence, the following results can be developed for  $\mathcal{C}_{\ell\ell}$ ,  $\mathcal{D}_{\phi\phi}$ , and  $\mathcal{C}_{\phi\ell}$ , namely that

$$\mathcal{C}_{\ell\ell}(p, m; p', m') = \frac{8.16}{4\pi} k^2 \int_0^Z dz C_N^2(z) [z(1-z/Z)/k]^{5/6} F(Q(p, m; p', m'; z)), \quad (26a)$$

$$\mathcal{D}_{\phi\phi}(p, m; p', m') = \frac{8.16}{2\pi} k^2 \int_0^Z dz C_N^2(z) [z(1-z/Z)/k]^{5/6} G(Q(p, m; p', m'; z)), \quad (26b)$$

$$\mathcal{C}_{\phi\ell}(p, m; p', m') = \frac{8.16}{4\pi} k^2 \int_0^Z dz C_N^2(z) [z(1-z/Z)/k]^{5/6} H(Q(p, m; p', m'; z)), \quad (26c)$$

where the notation  $Z$  denotes the range from the ground to the satellite (*i.e.* from the laser transmitter's aperture plane to the laser receiver or beacon source on the satellite), the variable of integration,  $z$ , can be considered to denote position along the propagation path (from  $z = 0$  at the ground to  $z = Z$  at the satellite), and  $C_N^2(z)$  denotes the value of the refractive index structure constant (which is a measure of the optical strength of turbulence) at the position  $z$  along the propagation path. The three functions  $F(Q)$ ,  $G(Q)$ , and  $H(Q)$  are defined by the equations

$$F(Q) = \int_0^\infty d\kappa \kappa^{-8/3} J_0(\kappa Q) [1 - \cos(\kappa^2)], \quad (27a)$$

$$G(Q) = \int_0^\infty d\kappa \kappa^{-8/3} [1 - J_0(\kappa Q)] [1 + \cos(\kappa^2)], \quad (27b)$$

$$H(Q) = \int_0^\infty d\kappa \kappa^{-8/3} J_0(\kappa Q) \sin(\kappa^2). \quad (27c)$$

The quantity  $Q(p, m; p', m'; z)$  appearing in Eq. (26) has a value given by the equation

$$Q(p, m; p', m'; z) = \frac{|\mathbf{r}_p - \mathbf{r}_{p'}| (1 - z/Z) + (\boldsymbol{\theta}_m - \boldsymbol{\theta}_{m'}) z - \mathbf{V}(z) (t_m - t_{m'})|}{\mathcal{L}_F}, \quad (28)$$

where  $\mathbf{V}(z)$  denotes the projection onto a plane parallel to the aperture plane of the vector representing the wind velocity that exists at the range  $z$ , where  $\boldsymbol{\theta}_m$  and  $\boldsymbol{\theta}_{m'}$  denote directions associated with arrival of the beacon's light at time  $t_m$  and  $t_{m'}$ , when  $m$  and/or  $m' = \{1, 2, 3, \dots, M\}$  and the direction associated with transmission to the satellite at time  $t_0$  when  $m$  and/or  $m' = 0$ , and where the quantity  $\mathcal{L}_F$ , which may be considered to be a sort of Fresnel length, has a value given by the equation

$$\mathcal{L}_F = \sqrt{\frac{kZ}{z(Z-z)}}. \quad (29)$$

An interesting physical interpretation can be placed on the definition of  $Q(p, m; p', m'; z)$  given by Eq. (28) —an interpretation as a separation length divided by the normalization length  $\mathcal{L}_F$ . To explain what I am referring to when I speak of a “separation length” I call attention to a pair of rays to/from the aperture plane. Ray-1 is associated with  $(p, m)$ , *i.e.* with the aperture plane position  $\mathbf{r}_p$ , the time  $t_m$ , and the direction  $\boldsymbol{\theta}_m$ . Ray-2 is associated with  $(p', m')$ , *i.e.* with the aperture plane position  $\mathbf{r}_{p'}$ , the time  $t_{m'}$ , and the direction  $\boldsymbol{\theta}_{m'}$ . In accordance with the Taylor hypothesis of frozen flow, we may consider the turbulence pattern *per se* to be unchanging with time but to be transported by the ambient wind. At time  $t_m$  Ray-1 pierces the turbulence pattern that exists at the range  $z$  —pierces it at some position. At time  $t_{m'}$  Ray-2 pierces this same turbulence pattern at some other position. It is then appropriate to ask what is the separation between where the first ray pierced the turbulence pattern and where the second ray pierced that pattern.

It can be seen that the rays pierce a fixed plane at range  $z$  at positions that are separated by  $(\mathbf{r}_p - \mathbf{r}_{p'}) (1 - z/Z) + (\boldsymbol{\theta}_m - \boldsymbol{\theta}_{m'}) z$ . But since the turbulence pattern has moved a distance  $\mathbf{V}(z) (t_m - t_{m'})$  in the time interval between the two piercings, the separation between where the turbulence pattern is pierced by these two rays is reduced by  $\mathbf{V}(z) (t_m - t_{m'})$ . Accordingly the separation of the two piercings of the turbulence pattern *per se* is given by the expression  $(\mathbf{r}_p - \mathbf{r}_{p'}) (1 - z/Z) + (\boldsymbol{\theta}_m - \boldsymbol{\theta}_{m'}) z - \mathbf{V}(z) (t_m - t_{m'})$  —which is the numerator of the fraction on the right-hand-side of Eq. (28).

Expressing the trigonometric functions in Eq. (27) in terms of a sum/difference of exponential functions and making use of well known results for certain definite integrals<sup>2</sup> it can be shown that the functions  $F(Q)$ ,  $G(Q)$ , and  $H(Q)$ , which are defined by Eq. (26), have values given by the equations

$$F(Q) = \frac{1}{2} \frac{\Gamma(-\frac{5}{6})}{\Gamma(\frac{11}{6})} \left(\frac{1}{4} Q^2\right)^{5/6} - \frac{1}{2} \Gamma(-\frac{5}{6}) \Re \left\{ \exp\left(\frac{5}{12} \pi i\right) {}_1F_1\left(-\frac{5}{6}; 1; \frac{1}{4} Q^2 i\right) \right\}, \quad (30a)$$

$$G(Q) = -\frac{1}{2} \frac{\Gamma(-\frac{5}{6})}{\Gamma(\frac{11}{6})} \left(\frac{1}{4} Q^2\right)^{5/6} - \frac{1}{2} \Gamma(-\frac{5}{6}) \left[ \Re \left\{ \exp\left(\frac{5}{12} \pi i\right) {}_1F_1\left(-\frac{5}{6}; 1; \frac{1}{4} Q^2 i\right) \right\} - \cos\left(\frac{5}{12} \pi\right) \right], \quad (30b)$$

$$H(Q) = \frac{1}{2} \Gamma(-\frac{5}{6}) \Re \left\{ \exp\left(\frac{11}{12} \pi i\right) {}_1F_1\left(-\frac{5}{6}; 1; \frac{1}{4} Q^2 i\right) \right\}. \quad (30c)$$

The hyper geometric functions appearing in this result can be evaluated using the standard power series formulation—so long as  $Q$  is not too large. With 16-digit computational accuracy quite accurate results can be developed for values of  $Q$  as large as  $Q = 10$ , but for values of  $Q$  much larger than about  $Q = 12$  the results obtained with 16-digit computational accuracy are very clearly in error. To circumvent this limitation/difficulty I have developed the asymptotic series results that

$$F(Q) = \frac{1}{4} \frac{\Gamma(\frac{7}{6})}{\Gamma(-\frac{1}{6})} \left(\frac{1}{4} Q^2\right)^{-7/6} - \frac{1}{2} \left(\frac{1}{4} Q^2\right)^{-11/6} \left[ 1 - \frac{8}{3} \frac{11}{3} \left(\frac{1}{4} Q^2\right)^{-2} + \frac{8}{3} \frac{11}{3} \frac{14}{3} \frac{17}{3} \left(\frac{1}{4} Q^2\right)^{-4} - \dots \right] \sin\left(\frac{1}{4} Q^2\right)$$

<sup>2</sup> I.S. Gradshteyn and I.M. Ryzhik, *Tables of Integrals, Series, and Products*, 4<sup>TH</sup> edition (Academic 1965 New York); Eq. (6.561.14), p. 684 and Eq. (6.631.1), p. 716

$$+ \frac{1}{2} \left( \frac{1}{4} Q^2 \right)^{-17/6} \left[ \frac{8}{3} - \frac{8}{3} \frac{11}{3} \frac{14}{3} \left( \frac{1}{4} Q^2 \right)^{-2} + \frac{8}{3} \frac{11}{3} \frac{14}{3} \frac{17}{3} \frac{20}{3} \left( \frac{1}{4} Q^2 \right)^{-4} - \dots \right] \cos \left( \frac{1}{4} Q^2 \right), \quad (31a)$$

$$G(Q) = -\frac{\Gamma\left(-\frac{5}{6}\right)}{\Gamma\left(\frac{11}{6}\right)} \left( \frac{1}{4} Q^2 \right)^{5/6} + F(Q) + \frac{1}{2} \Gamma\left(-\frac{5}{6}\right) \cos\left(\frac{5}{12} \pi\right), \quad (31b)$$

$$H(Q) = \frac{1}{2} \frac{\Gamma\left(\frac{1}{6}\right)}{\Gamma\left(\frac{5}{6}\right)} \left( \frac{1}{4} Q^2 \right)^{-1/6} + \frac{1}{2} \left( \frac{1}{4} Q^2 \right)^{-11/6} \left[ 1 - \frac{8}{3} \frac{11}{3} \left( \frac{1}{4} Q^2 \right)^{-2} + \frac{8}{3} \frac{11}{3} \frac{14}{3} \frac{17}{3} \left( \frac{1}{4} Q^2 \right)^{-4} - \dots \right] \cos\left(\frac{1}{4} Q^2\right) \\ + \frac{1}{2} \left( \frac{1}{4} Q^2 \right)^{-17/6} \left[ \frac{8}{3} - \frac{8}{3} \frac{11}{3} \frac{14}{3} \left( \frac{1}{4} Q^2 \right)^{-2} + \frac{8}{3} \frac{11}{3} \frac{14}{3} \frac{17}{3} \frac{20}{3} \left( \frac{1}{4} Q^2 \right)^{-4} - \dots \right] \sin\left(\frac{1}{4} Q^2\right), \quad (31c)$$

which results<sup>3</sup> very smoothly joint the results given by Eq. (30) at  $Q = 10$ .

Before closing this sub section I introduce one additional fact. Based on the presumption that the turbulence induced log-amplitude perturbations are normally distributed it can be shown by consideration of conservation of energy requirements, that

$$\bar{\ell} = -\mathcal{C}_{\ell\ell}(p, m; p, m) = -\mathcal{R}_{\mathcal{Y}}, \quad (32)$$

where the notation  $\mathcal{R}_{\mathcal{Y}}$  is used to denote what has come to be called the Rytov-number.<sup>4, 5</sup>

Having now provided all the computational formulations needed to develop Rytov approximation based second moment propagation statistics for the turbulence induced random phase and log-amplitude perturbations,  $\phi_{p,m}$  and  $\ell_{p,0}$ , I turn in the last of these three sub sections to the matter of applying these formulations in evaluation of the covariances and cross-covariances for the adjusted phase and adjusted log-amplitude perturbations,  $\tilde{\phi}_{p,m}$  and  $\tilde{\ell}_{p,0}$ .

### 3.3. Using The Rytov Approximation Results In Generating Covariance And Cross-Covariance Results For The Adjusted Phase And Adjusted Log-Amplitude Perturbations

It is obvious that this quantity,  $\tilde{\phi}_{p,m}$ , has a zero mean value. The covariance for this quantity,  $\mathcal{C}_{\tilde{\phi}\tilde{\phi}}(p, m; p', m')$ , may accordingly be considered to be defined by the equation

$$\mathcal{C}_{\tilde{\phi}\tilde{\phi}}(p, m; p', m') = \langle \tilde{\phi}_{p,m} \tilde{\phi}_{p',m'} \rangle. \quad (33)$$

An expression allowing evaluation of the value of this quantity can be easily developed using the simple algebraic relationship that  $(a - b)(c - d) = \frac{1}{2} [ -(a - c)^2 + (a - d)^2 + (b - c)^2 - (b - d)^2 ]$ . It follows from this and the definition of the phase structure function,  $\mathcal{D}_{\phi\phi}$ , given by Eq. (25b) that

$$\mathcal{C}_{\tilde{\phi}\tilde{\phi}}(p, m; p', m') = \frac{1}{2} [ -\mathcal{D}_{\phi\phi}(p, m; p', m') + \mathcal{D}_{\phi\phi}(p, m; 0, m') \\ + \mathcal{D}_{\phi\phi}(0, m; p', m') - \mathcal{D}_{\phi\phi}(0, m; 0, m') ]. \quad (34)$$

---

<sup>3</sup> The details of the derivation of these asymptotic series results would take up too much space to be worth presenting here. Details will be provided on request as my Tech-Note TN-205.

<sup>4</sup> D.L. Fried, "Scaling Laws for Propagation through Turbulence," Atmos. Oceanic Opt. **11** 982-990 (1998)

<sup>5</sup> I use the notation  $\mathcal{R}_{\mathcal{Y}}$  here, in place of the more customary notation  $\sigma_{\ell}^2$  (or  $\sigma_{\chi}^2$ ), called the log-amplitude variance, to take account of the fact that under propagation conditions for which  $\mathcal{R}$  is calculated to have a value larger than about  $\mathcal{R} = 0.25$  Np<sup>2</sup> there occurs what is called "saturation of scintillation" and the actual variance of the log-amplitude does not increase with increasing strength of turbulence.

Since  $\tilde{\phi}_{p,m}$  and  $\tilde{\ell}_{p',m'}$  each have mean values of zero their cross-covariance,  $\mathcal{C}_{\tilde{\phi}\tilde{\ell}}(p, m; p', m')$  can be considered to be defined by the equation

$$\mathcal{C}_{\tilde{\phi}\tilde{\ell}}(p, m; p', m') = \langle \tilde{\phi}_{p,m} \tilde{\ell}_{p',m'} \rangle. \quad (35)$$

Taking note of Eq.'s (11), (13), and (25c) it can be seen that

$$\mathcal{C}_{\tilde{\phi}\tilde{\ell}}(p, m; p', m') = \mathcal{C}_{\phi\ell}(p, m; p', m') - \mathcal{C}_{\phi\ell}(0, m; p', m'). \quad (36)$$

Since the mean value of  $\tilde{\ell}_{p,m}$  is zero the covariance for a pair of adjusted log-amplitude perturbation values, for say  $\ell_{p,m}$  and  $\ell_{p',m'}$ , which covariance I shall denote by the notation  $\mathcal{C}_{\tilde{\ell}\tilde{\ell}}(p, m; p', m')$ , may be considered to be defined by the equation

$$\mathcal{C}_{\tilde{\ell}\tilde{\ell}}(p, m; p', m') = \langle \tilde{\ell}_{p,m} \tilde{\ell}_{p',m'} \rangle. \quad (37)$$

Taking note of Eq.'s (13) and (25a) I see that I can write

$$\mathcal{C}_{\tilde{\ell}\tilde{\ell}}(p, m; p', m') = \mathcal{C}_{\ell\ell}(p, m; p', m'). \quad (38)$$

With Eq.'s (34), (36), and (38) along with Eq. (32) in hand I have expressions for evaluation of all the elements of the covariance matrix,  $\mathbf{C}_z$ , when the elements of  $\mathbf{z}$  correspond to the adjusted phase and adjusted log-amplitude perturbations,  $\tilde{\phi}_{p,m}$  and  $\tilde{\ell}_{p,m}$ . With such a covariance matrix I can generate statistically appropriate random realizations for the values of  $\tilde{\phi}_{p,m}$  and  $\tilde{\ell}_{p,m}$ —and from this can generate statistically appropriate random realizations of the Up-Link Strehl ratio,  $\mathcal{S}$ .

Unfortunately, because many prior times,  $t_m$  for  $m = \{1, 2, 3, \dots, M\}$  are generally required to allow proper simulation of the tilt tracking process that is represented by Eq. (8), the size of the required covariance matrix,  $\mathbf{C}_z$ , can be awkwardly large. To avoid this difficulty, in the next section I shall consider the possibility of making the beacon tilts at time  $t_m$ , namely  $\vartheta_m^x$  and  $\vartheta_m^y$ , elements of the column vector  $\mathbf{z}$  and developing statistically appropriate randomly selected values for these quantities directly from application of Eq. (22). This would allow me to drop the task of generating  $P \times M$  of the prior time adjusted phase perturbation,  $\tilde{\phi}_{p,m}$ , random values, dropping these elements from the column vector  $\mathbf{z}$ —generating in their place only  $2M$  random tilt values values,  $\vartheta_m^x$  and  $\vartheta_m^y$ —thus greatly reducing the length of  $\mathbf{z}$  and the size of its covariance matrix,  $\mathbf{C}_z$ .

#### 4. Directly Generating Prior Time Beacon Tilt Random Values

If the  $\vartheta_m^x$  and  $\vartheta_m^y$  random quantities are to be elements of  $\mathbf{z}$  then I will need expressions allowing evaluation of the following covariances and cross-covariances, namely

$$\mathcal{C}_{xx}(m; m') = \langle \vartheta_m^x \vartheta_{m'}^x \rangle, \quad (39a)$$

$$\mathcal{C}_{xy}(m; m') = \langle \vartheta_m^x \vartheta_{m'}^y \rangle, \quad (39b)$$

$$\mathcal{C}_{yy}(m; m') = \langle \vartheta_m^y \vartheta_{m'}^y \rangle, \quad (39c)$$

$$\mathcal{C}_{\tilde{\phi}X}(p, m; m') = \langle \tilde{\phi}_{p,m} \vartheta_{m'}^X \rangle, \quad (39d)$$

$$\mathcal{C}_{\tilde{\phi}Y}(p, m; m') = \langle \tilde{\phi}_{p,m} \vartheta_{m'}^Y \rangle, \quad (39e)$$

$$\mathcal{C}_{\tilde{\ell}X}(p, m; m') = \langle \tilde{\ell}_{p,m} \vartheta_{m'}^X \rangle, \quad (39f)$$

$$\mathcal{C}_{\tilde{\ell}Y}(p, m; m') = \langle \tilde{\ell}_{p,m} \vartheta_{m'}^Y \rangle. \quad (39g)$$

Substituting from Eq. (10) into Eq. (39a), making a double sum of the product of two sums (using  $p$  as the summation index for one of the sums and  $p'$  as the summation index for the other summation), then interchanging the order of summation and of ensemble averaging, and finally making use of Eq. (33) and then of Eq. (34), I can write for  $\mathcal{C}_{XX}(m; m')$  that

$$\begin{aligned} \mathcal{C}_{XX}(m; m') &= k^{-2} \left\langle \sum_{p=1}^P \tilde{x}_p \tilde{\phi}_{p,m} \sum_{p'=1}^P \tilde{x}_{p'} \tilde{\phi}_{p',m'} \right\rangle \\ &= k^{-2} \left\langle \sum_{p,p'=1}^P \tilde{x}_p \tilde{x}_{p'} \tilde{\phi}_{p,m} \tilde{\phi}_{p',m'} \right\rangle \\ &= k^{-2} \sum_{p,p'=1}^P \tilde{x}_p \tilde{x}_{p'} \langle \tilde{\phi}_{p,m} \tilde{\phi}_{p',m'} \rangle \\ &= k^{-2} \sum_{p,p'=1}^P \tilde{x}_p \tilde{x}_{p'} \mathcal{C}_{\tilde{\phi}\tilde{\phi}}(p, m; p', m') \\ &= k^{-2} \sum_{p,p'=1}^P \tilde{x}_p \tilde{x}_{p'} \{ -\mathcal{D}_{\phi\phi}(p, m; p', m') + \mathcal{D}_{\phi\phi}(p, m; 0, m') \\ &\quad + \mathcal{D}_{\phi\phi}(0, m; p', m') - \mathcal{D}_{\phi\phi}(0, m; 0, m) \}. \end{aligned} \quad (40)$$

Proceeding similarly for  $\mathcal{C}_{XY}(m; m')$  and  $\mathcal{C}_{YY}(m; m')$  I obtain the results that

$$\begin{aligned} \mathcal{C}_{XY}(m; m') &= k^{-2} \sum_{p,p'=1}^P \tilde{x}_p \tilde{y}_{p'} \{ -\mathcal{D}_{\phi\phi}(p, m; p', m') + \mathcal{D}_{\phi\phi}(p, m; 0, m') \\ &\quad + \mathcal{D}_{\phi\phi}(0, m; p', m') - \mathcal{D}_{\phi\phi}(0, m; 0, m) \}, \end{aligned} \quad (41)$$

and

$$\begin{aligned} \mathcal{C}_{YY}(m; m') &= k^{-2} \sum_{p,p'=1}^P \tilde{y}_p \tilde{y}_{p'} \{ -\mathcal{D}_{\phi\phi}(p, m; p', m') + \mathcal{D}_{\phi\phi}(p, m; 0, m') \\ &\quad + \mathcal{D}_{\phi\phi}(0, m; p', m') - \mathcal{D}_{\phi\phi}(0, m; 0, m) \}. \end{aligned} \quad (42)$$

Following the same general sort of analytic development as was used in developing Eq. (40) I can write for  $\mathcal{C}_{\tilde{\phi}X}(p, m; m')$  that

$$\mathcal{C}_{\tilde{\phi}X}(p, m; m') = k^{-1} \left\langle \tilde{\phi}_{p,m} \sum_{p'=1}^P \tilde{x}_{p'} \tilde{\phi}_{p',m'} \right\rangle$$



$$\begin{aligned}
&= k^{-1} \left\langle \sum_{p'=1}^P \tilde{x}_{p'} \tilde{\phi}_{p,m} \tilde{\phi}_{p',m'} \right\rangle \\
&= k^{-1} \sum_{p'=1}^P \tilde{x}_{p'} \langle \tilde{\phi}_{p,m} \tilde{\phi}_{p',m'} \rangle \\
&= k^{-1} \sum_{p'=1}^P \tilde{x}_{p'} \mathcal{C}_{\tilde{\phi}\tilde{\phi}}(p, m; p', m') \\
&= k^{-1} \sum_{p'=1}^P \tilde{x}_{p'} \{ -\mathcal{D}_{\phi\phi}(p, m; p', m') + \mathcal{D}_{\phi\phi}(p, m; 0, m') \\
&\quad + \mathcal{D}_{\phi\phi}(0, m; p', m') - \mathcal{D}_{\phi\phi}(0, m; 0, m) \}. \tag{43}
\end{aligned}$$

The corresponding result for  $\mathcal{C}_{\tilde{\phi}_Y}(p, m; m')$  is

$$\begin{aligned}
\mathcal{C}_{\tilde{\phi}_Y}(p, m; m') &= k^{-1} \sum_{p'=1}^P \tilde{y}_{p'} \{ -\mathcal{D}_{\phi\phi}(p, m; p', m') + \mathcal{D}_{\phi\phi}(p, m; 0, m') \\
&\quad + \mathcal{D}_{\phi\phi}(0, m; p', m') - \mathcal{D}_{\phi\phi}(0, m; 0, m) \}. \tag{44}
\end{aligned}$$

Proceeding in essentially the same way for the evaluation of  $\mathcal{C}_{\tilde{\ell}_X}(p, m; m')$ , only this time making use of Eq. (35) rather than Eq. (33) and Eq. (36) rather than Eq. (34), I write

$$\begin{aligned}
\mathcal{C}_{\tilde{\ell}_X}(p, m; m') &= k^{-1} \left\langle \tilde{\ell}_{p,m} \sum_{p'=1}^P \tilde{x}_{p'} \tilde{\phi}_{p',m'} \right\rangle \\
&= k^{-1} \left\langle \sum_{p'=1}^P \tilde{x}_{p'} \tilde{\ell}_{p,m} \tilde{\phi}_{p',m'} \right\rangle \\
&= k^{-1} \sum_{p'=1}^P \tilde{x}_{p'} \langle \tilde{\ell}_{p,m} \tilde{\phi}_{p',m'} \rangle \\
&= k^{-1} \sum_{p'=1}^P \tilde{x}_{p'} \mathcal{C}_{\tilde{\phi}\tilde{\ell}}(p', m'; p, m) \\
&= k^{-1} \sum_{p'=1}^P \tilde{x}_{p'} \{ \mathcal{C}_{\phi\ell}(p', m'; p, m) - \mathcal{C}_{\phi\ell}(0, m'; p, m) \}. \tag{45}
\end{aligned}$$

The corresponding result for  $\mathcal{C}_{\tilde{\ell}_Y}(p, m; m')$  is

$$\mathcal{C}_{\tilde{\ell}_Y}(p, m; m') = k^{-1} \sum_{p'=1}^P \tilde{y}_{p'} \{ \mathcal{C}_{\phi\ell}(p', m'; p, m) - \mathcal{C}_{\phi\ell}(0, m'; p, m) \}. \tag{46}$$

With these results in hand I can now consider a version of  $\mathbf{z}$ , the column vector of random variables, that consist of

- of  $P$  values for the current time phase,  $\tilde{\phi}_{p,0}$ ,
- of  $P$  values for the current time log-amplitude,  $\tilde{\ell}_{p,0}$ ,
- of  $M$  values for the prior times x-components of tilt,  $\vartheta_m^x$ , and
- of  $M$  values for the prior times y-components of tilt,  $\vartheta_m^y$ ,

a total of  $2(P + M)$  random values needed to generate a Strehl ratio value when the prior time tilts are generated directly rather than calculated from all of the prior time adjusted phases values. This number,  $2(P + M)$ , is considerably less than the  $P(M + 2)$  number of elements—  $P(1 + M)$  for the current time and all the prior time adjusted phase perturbation values and  $P$  for the current time adjusted log-amplitude perturbation values—that would have had to have been generated if the prior time tilts were calculated from directly generated prior time adjusted phase perturbation values. In terms of the covariance matrix and the computational time charge for extraction of its eigen vectors and eigen values this is a very important reduction in matrix size. It is also a significant factor in terms of the time required for generation of each random realization of the Strehl ratio's value, particularly if millions of random realizations are required—as in the development of results relating to low probability of occurrence Strehl ratio values.

With all of the needed computational tools defining RytovProp now in place I turn in the next section to a presentation of results demonstrating the soundness of the RytovProp method. I will present sample results generated using this method and compare these results with results generated utilizing the wave optics propagation simulation methods.

## 5. Testing/Validation Of The RytovProp Method

To allow an assessment of the soundness of the results produced by RytovProp I have compared results produced using RytovProp with corresponding results<sup>6</sup> produced using the split-step wave optics propagation simulation method, for the Up-Link Strehl ratio. There were a total of 66 different engagements for which results were prepared. These engagements differed in terms of 1) the satellite's altitude, 2) the zenith angle, 3) the optical wave length, 4) the aperture diameter, and 5) the optical strength of turbulence. The satellite altitudes that were considered were 400 km, 1500 km, and that corresponding to a geo synchronous orbit. The propagation directions that were considered were straight up (*i.e.* with a zenith angle of 0 rad) and at  $45^\circ$  to the zenith direction (*i.e.* with a zenith angle of  $\frac{1}{4}\pi$  rad). The optical wave lengths that were considered were  $\lambda = 0.5 \mu\text{m}$  and  $\lambda = 1.5 \mu\text{m}$ . The aperture diameters that were considered were  $D = 0.1 \text{ m}$  and  $D = 0.25 \text{ m}$ . (There were wave optics propagation results developed for a diameter of  $D = 0.5 \text{ m}$ , but these results were not used in the comparison tests being reported here. The optical strengths of turbulence that were used matched the  $\text{HV}_{5/7}$  turbulence model—but either scaled to match the best 10% integrated strength observed at the Starfire Optical Range, or at its nominal values (*i.e.* not scaled), or scaled to match the worst 10% integrated strength observed at the Starfire Optical Range.

For each engagement three separate sets of results were developed, one set for a ground system having a tilt tracking servo bandwidths of 0 Hz (no tilt tracking), one for a ground system with a tilt tracking servo bandwidth of 3 Hz, and one set for a ground system having a tilt tracking servo bandwidths of 10 Hz.

---

<sup>6</sup> These results were prepared by Barry Foucault at SAIC.

The split-step wave optics propagation simulations were all run with a frame rate of 3,000 frames per second. These simulations were run in sequences of 2,800 frames, with the first 700 frames of each sequence being discarded as being “contaminated” by tilt tracking servo start-up transients. For each such 2,800 frame sequence there was a single random number seed used in generating the simulated turbulence patterns that were used—a random number seed that was unique to that sequence of 2,800 frames. For each of the 66 engagements treated there were several such sequences of 2,100 usable frames of data (*i.e.* Strehl ratio values) generated, but in the largest cases there were only 20 such sequences generated—yielding a total of only 42,000 Strehl ratio values.

It is inherent in the way the split-step wave optics propagation simulation process is (normally) used that there is in general very little change in the turbulence pattern from frame to frame. As a consequence there is a high degree of correlation between successive Strehl ratio values produced. In studying the frame-to-frame correlation of Strehl ratio values I found that in general the correlation dropped to a normalized value of about one-half with a separation of the order of ten frames—indicating that there actually were no more than about 4,000 degrees-of-freedom in any one of the 66 cases.

The corresponding sets of RytovProp based results each had 100,000 statistically independent Strehl Ratio values. (It is inherent in the RytovProp method that, unless special steps are taken to obtain results with some degree of correlation, there will be no correlation between any two Strehl ratio values in a set.) Accordingly there are 100,000 degrees-of-freedom in the RytovProp results I am presenting.

Cumulative probability distribution results were developed for each of the 66 engagement scenarios. Separate cumulative probability distribution results for each of the three tilt tracking servo bandwidths were developed—both from the set of Strehl ratio values obtained using the split-step wave optics propagation simulation method and from the set of Strehl ratio results obtained using the RytovProp method. In general there appeared to be good agreement between the two sets of results, but with some quite noticeable discrepancies between the two sets of results in the low probability range—to some extent the below 1.0% range but more so in the below 0.1% range. I attribute such discrepancies to the relatively small number of degrees-of-freedom in the sets of Strehl ratio values produced using the split-step wave optics propagation simulation method.

To illustrate this situation in Fig.’s 1, 2, and 3 I show the cumulative probability distribution results for aperture diameters of  $D = 0.1$  m and  $D = 0.25$  m, and for wave lengths of  $\lambda = 0.5 \mu\text{m}$  and  $\lambda = 1.5 \mu\text{m}$ . The results shown in these three figures were chosen from the 66 different engagement scenarios studied, were chosen for presentation here on the basis that they are for engagements for which the values of the Rytov number—for optical wave length of  $\lambda = 0.5 \mu\text{m}$ —is about  $\mathcal{R}_y = 0.3 \text{ Np}^2$ ,  $\mathcal{R}_y = 0.1 \text{ Np}^2$ , and  $\mathcal{R}_y = 0.03 \text{ Np}^2$ . For Fig. 1, *i.e.* for the first engagement scenario, the value of the Rytov number for wave lengths of  $\lambda = 0.5 \mu\text{m}$  (and  $\lambda = 1.5 \mu\text{m}$ ) is  $\mathcal{R}_y = 0.3262 \text{ Np}^2$  (and  $\mathcal{R}_y = 0.0905 \text{ Np}^2$ ), while the effective coherence diameter has a value of  $r_o = 0.017$  m (and  $r_o = 0.063$  m), with the Tyler frequency having a value of  $f_T = 56.7$  Hz (and  $f_T = 18.9$  Hz). For Fig. 2, *i.e.* for the second engagement scenario, the value of the Rytov number for wave lengths of  $\lambda = 0.5 \mu\text{m}$  (and  $\lambda = 1.5 \mu\text{m}$ ) is  $\mathcal{R}_y = 0.1028 \text{ Np}^2$  (and  $\mathcal{R}_y = 0.0285 \text{ Np}^2$ ), while the effective coherence diameter has a value of  $r_o = 0.042$  m (and  $r_o = 0.158$  m), with the Tyler frequency having a value of  $f_T = 28.1$  Hz (and  $f_T = 9.4$  Hz). For Fig. 3, *i.e.* for the third engagement scenario, the value of the Rytov number for wave lengths of  $\lambda = 0.5 \mu\text{m}$  (and  $\lambda = 1.5 \mu\text{m}$ ) is  $\mathcal{R}_y = 0.0326 \text{ Np}^2$  (and  $\mathcal{R}_y = 0.0091 \text{ Np}^2$ ), while the effective coherence diameter has a value of  $r_o = 0.103$  m (and  $r_o = 0.386$  m), with the Tyler frequency having a value of  $f_T = 16.8$  Hz (and  $f_T = 5.6$  Hz).

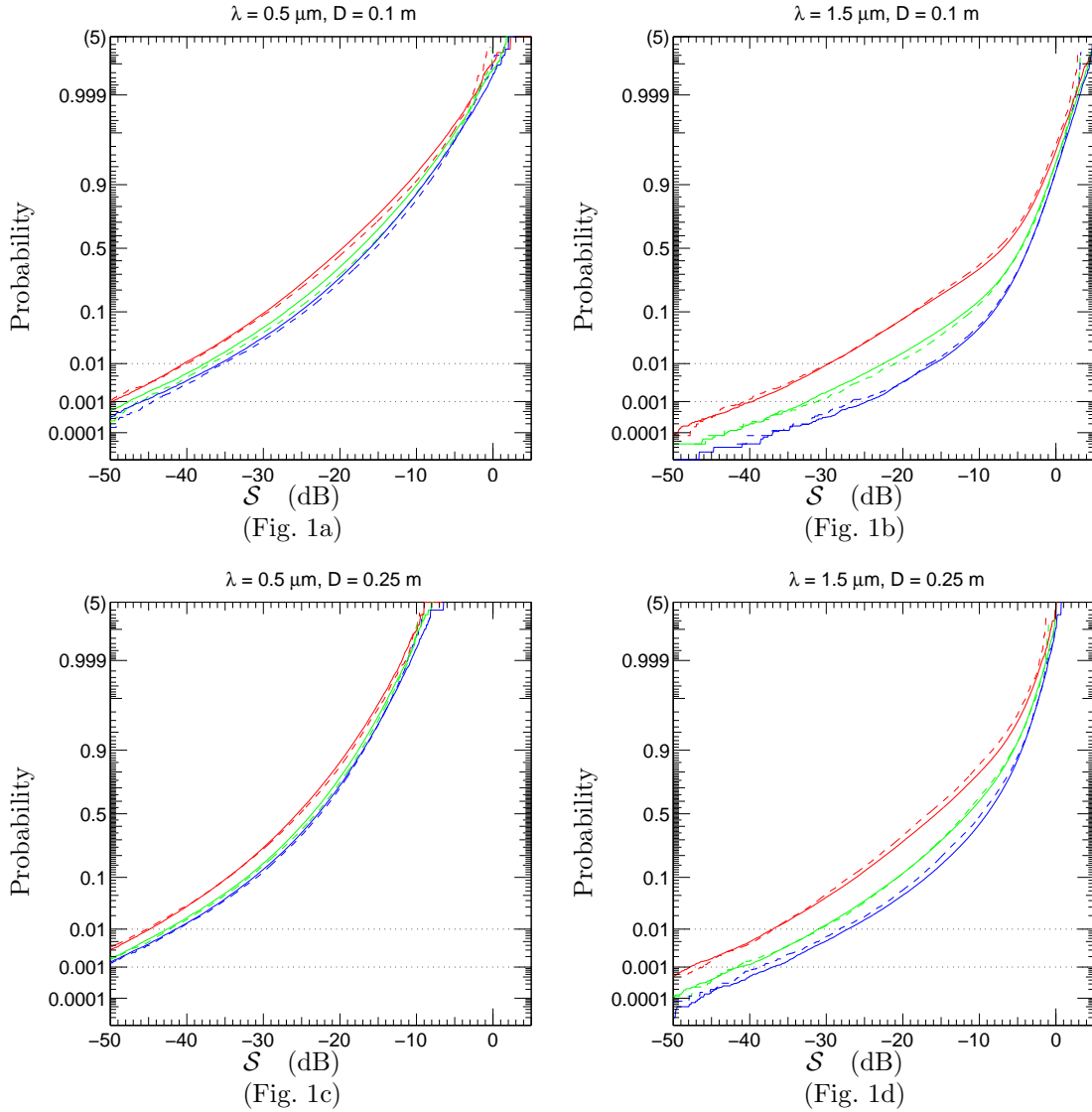


Figure 1. Cumulative Probability Distribution For The First Engagement Scenario

Each of the four plots is for the combinations of aperture diameter,  $D$ , and optical wave length,  $\lambda$ , indicated above that plot. The engagement parameters are such that for  $\lambda = 0.5 \mu\text{m}$  the relevant turbulence parameters have values of  $\mathcal{R}_y = 0.3262 \text{ Np}^2$ ,  $r_o = 0.017 \text{ m}$ , and  $f_T = 56.7 \text{ Hz}$ , while for  $\lambda = 1.5 \mu\text{m}$  the values are  $\mathcal{R}_y = 0.0905 \text{ Np}^2$ ,  $r_o = 0.063 \text{ m}$ , and  $f_T = 18.9 \text{ Hz}$ . The dashed line curves show the results obtained using the split-step wave optics propagation simulation method. The solid line curves show the results obtained using the RytovProp method. The red line curves are for the case where the tilt tracking servo bandwidth was  $f_{3\text{dB}} = 0 \text{ Hz}$ , while the green line and the blue line curves are for  $f_{3\text{dB}} = 3 \text{ Hz}$  and  $f_{3\text{dB}} = 10 \text{ Hz}$  respectively. The horizontal dotted lines indicate the 1% and the 0.1% cumulative probability levels.

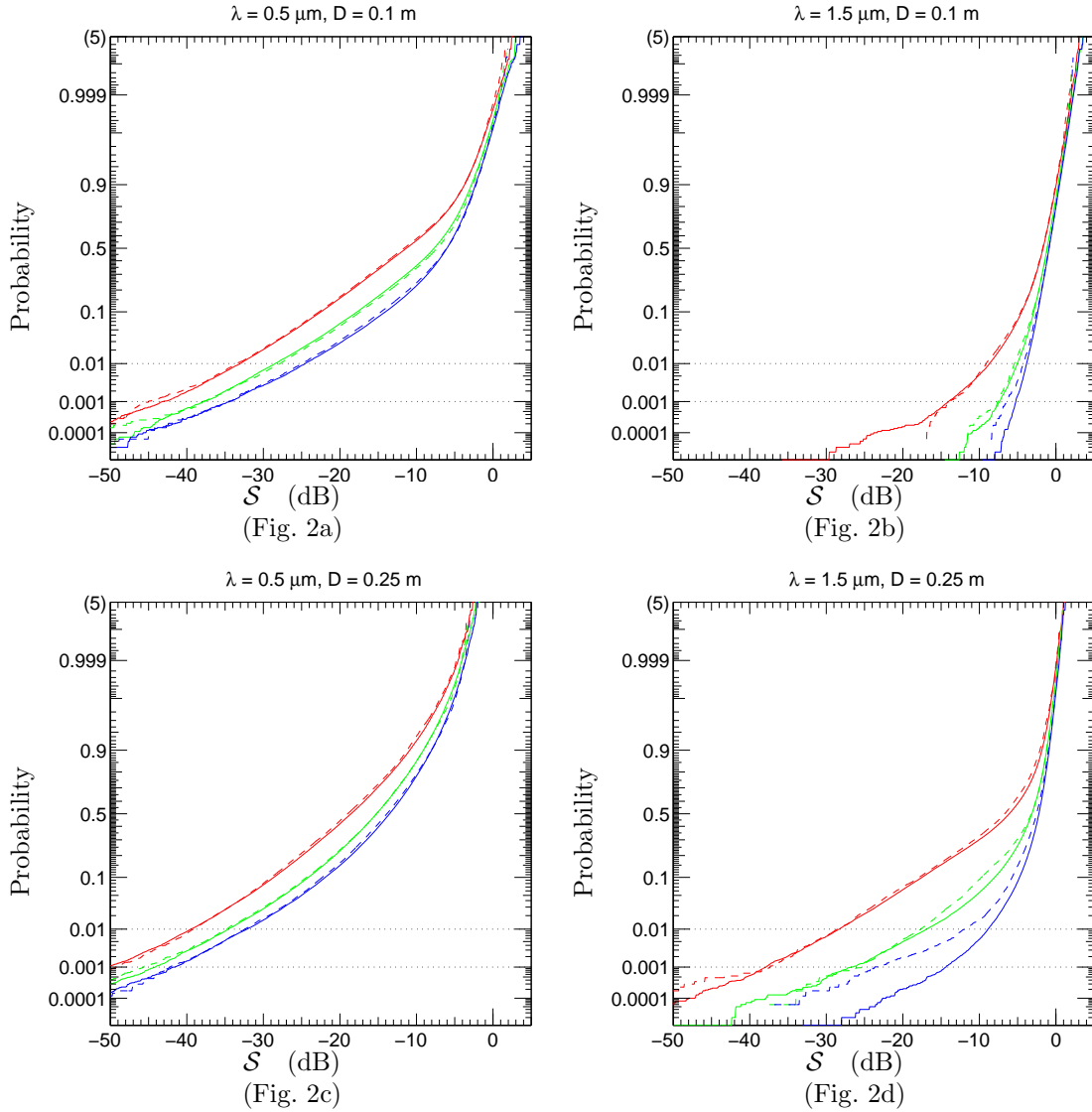


Figure 2. Cumulative Probability Distribution For The First Engagement Scenario

Each of the four plots is for the combinations of aperture diameter,  $D$ , and optical wave length,  $\lambda$ , indicated above that plot. The engagement parameters are such that for  $\lambda = 0.5 \mu\text{m}$  the relevant turbulence parameters have values of  $\mathcal{R}_y = 0.103 \text{ Np}^2$ ,  $r_0 = 0.042 \text{ m}$ , and  $f_T = 28.1 \text{ Hz}$ , while for  $\lambda = 1.5 \mu\text{m}$  the values are  $\mathcal{R}_y = 0.029 \text{ Np}^2$ ,  $r_0 = 0.158 \text{ m}$ , and  $f_T = 9.4 \text{ Hz}$ . The dashed line curves show the results obtained using the split-step wave optics propagation simulation method. The solid line curves show the results obtained using the RytovProp method. The red line curves are for the case where the tilt tracking servo bandwidth was  $f_{3\text{dB}} = 0 \text{ Hz}$ , while the green line and the blue line curves are for  $f_{3\text{dB}} = 3 \text{ Hz}$  and  $f_{3\text{dB}} = 10 \text{ Hz}$  respectively. The horizontal dotted lines indicate the 1% and the 0.1% cumulative probability levels.

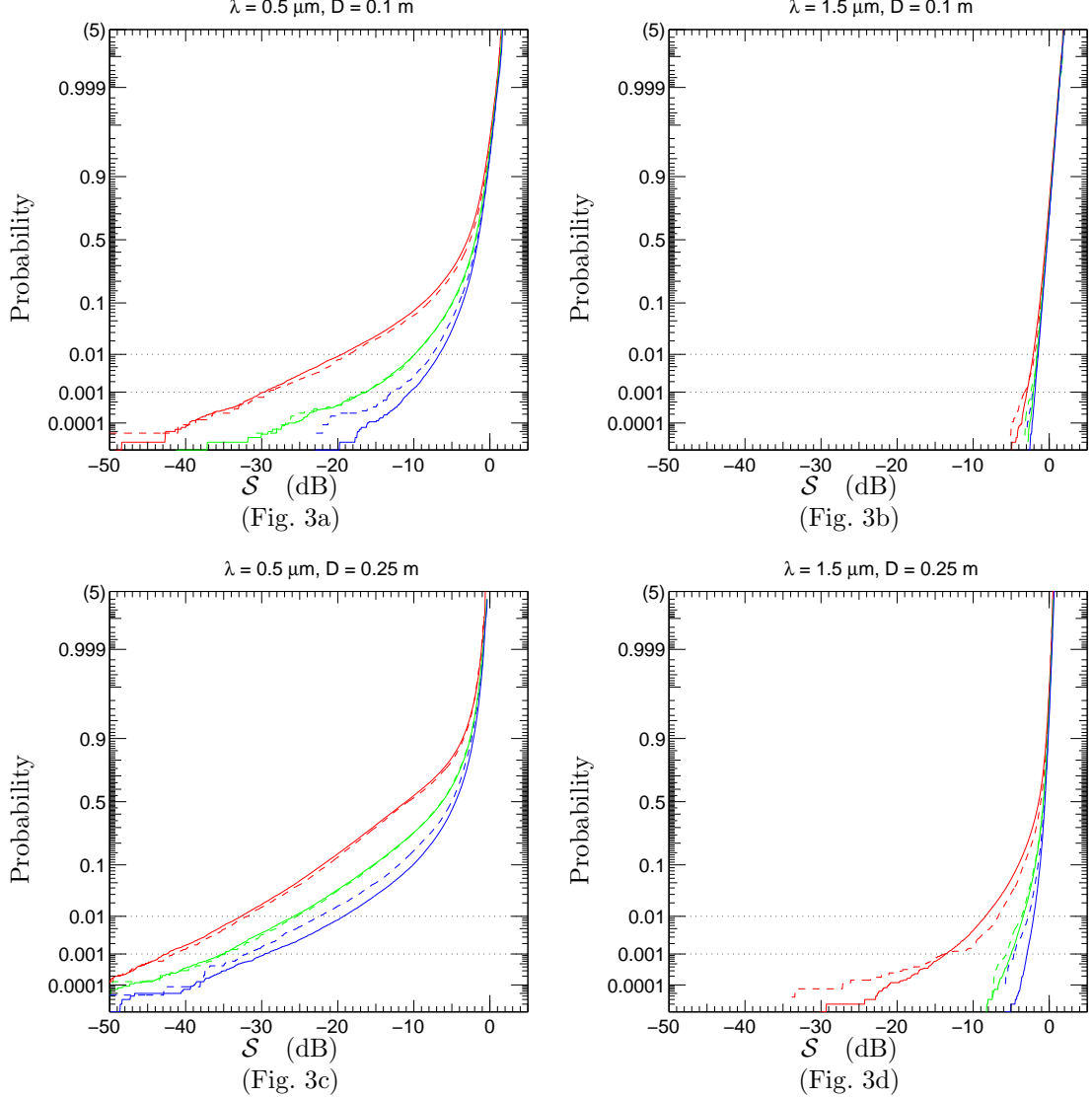


Figure 3. Cumulative Probability Distribution For The First Engagement Scenario

Each of the four plots is for the combinations of aperture diameter,  $D$ , and optical wave length,  $\lambda$ , indicated above that plot. The engagement parameters are such that for  $\lambda = 0.5 \mu\text{m}$  the relevant turbulence parameters have values of  $\mathcal{R}_y = 0.033 \text{ Np}^2$ ,  $r_0 = 0.103 \text{ m}$ , and  $f_T = 16.8 \text{ Hz}$ , while for  $\lambda = 1.5 \mu\text{m}$  the values are  $\mathcal{R}_y = 0.009 \text{ Np}^2$ ,  $r_0 = 0.386 \text{ m}$ , and  $f_T = 5.6 \text{ Hz}$ . The dashed line curves show the results obtained using the split-step wave optics propagation simulation method. The solid line curves show the results obtained using the RytovProp method. The red line curves are for the case where the tilt tracking servo bandwidth was  $f_{3\text{dB}} = 0 \text{ Hz}$ , while the green line and the blue line curves are for  $f_{3\text{dB}} = 3 \text{ Hz}$  and  $f_{3\text{dB}} = 10 \text{ Hz}$  respectively. The horizontal dotted lines indicate the 1% and the 0.1% cumulative probability levels.

To help in judging the significance of what discrepancies can be seen in these figures—which discrepancies I believe are almost entirely inherent in the dashed line curves and are due to the smallness of the number of degrees-of-freedom in the sets of split-step wave optics propagation simulation Strehl ratio values used in forming each of those dashed line curves—one needs to consider not only the total number of the Strehl ratio values in each set, but also the degree of correlation of the successive Strehl ratio values.

For Fig.'s. 1a and 1c there were 39,900 Strehl ratio values used in forming the dashed line curves, while for Fig.'s 1b and 1d there were 25,200 Strehl ratio values used. For Fig.'s 2a and 2c there were 33,600 Strehl ratio values used in forming the dashed line curves, while for Fig.'s 2b and 2d there were 16,800 Strehl ratio values used. For Fig.'s 3a and 3c there were 23,100 Strehl ratio values used in forming the dashed line curves, while for Fig.'s 3b and 3d there were 27,300 Strehl ratio values used.

To provide information about the correlation of successive Strehl ratio values produced by the split-step wave optics propagation method in Fig.'s 4, 5, and 6 I show the correlation of these successive Strehl ratio values for the data sets used in generating the curves shown in Fig.'s 1, 2, and 3 respectively.

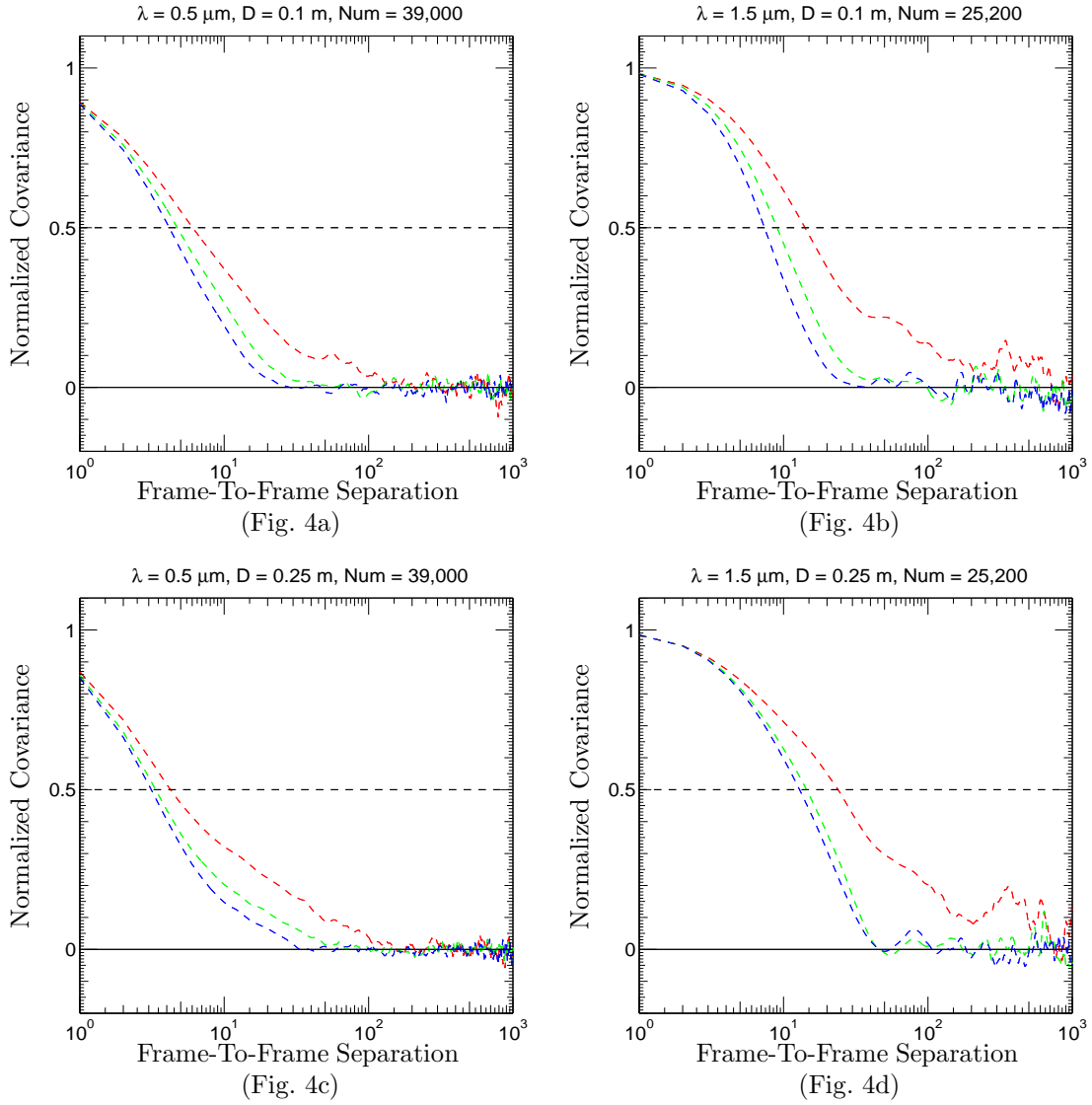


Figure 4. Normalized Correlation Of Successive Strehl Ratio Values

The three curves in each plot are to be associated with the similarly colored dashed line curves in the corresponding plots of Fig. 1 —the curves based on the wave optics propagation method. The normalized covariance is the covariance divided by the variance. The notation Num above each plot indicates the number of Strehl ratio values were used in producing the results shown in Fig. 1. The value of Num divided by the Frame-to-Frame Separation at which the normalized covariance curve crosses the 0.5 level can be taken as an estimate of the number of degrees-of-freedom in the data used forming the dashed line curves of Fig. 1.



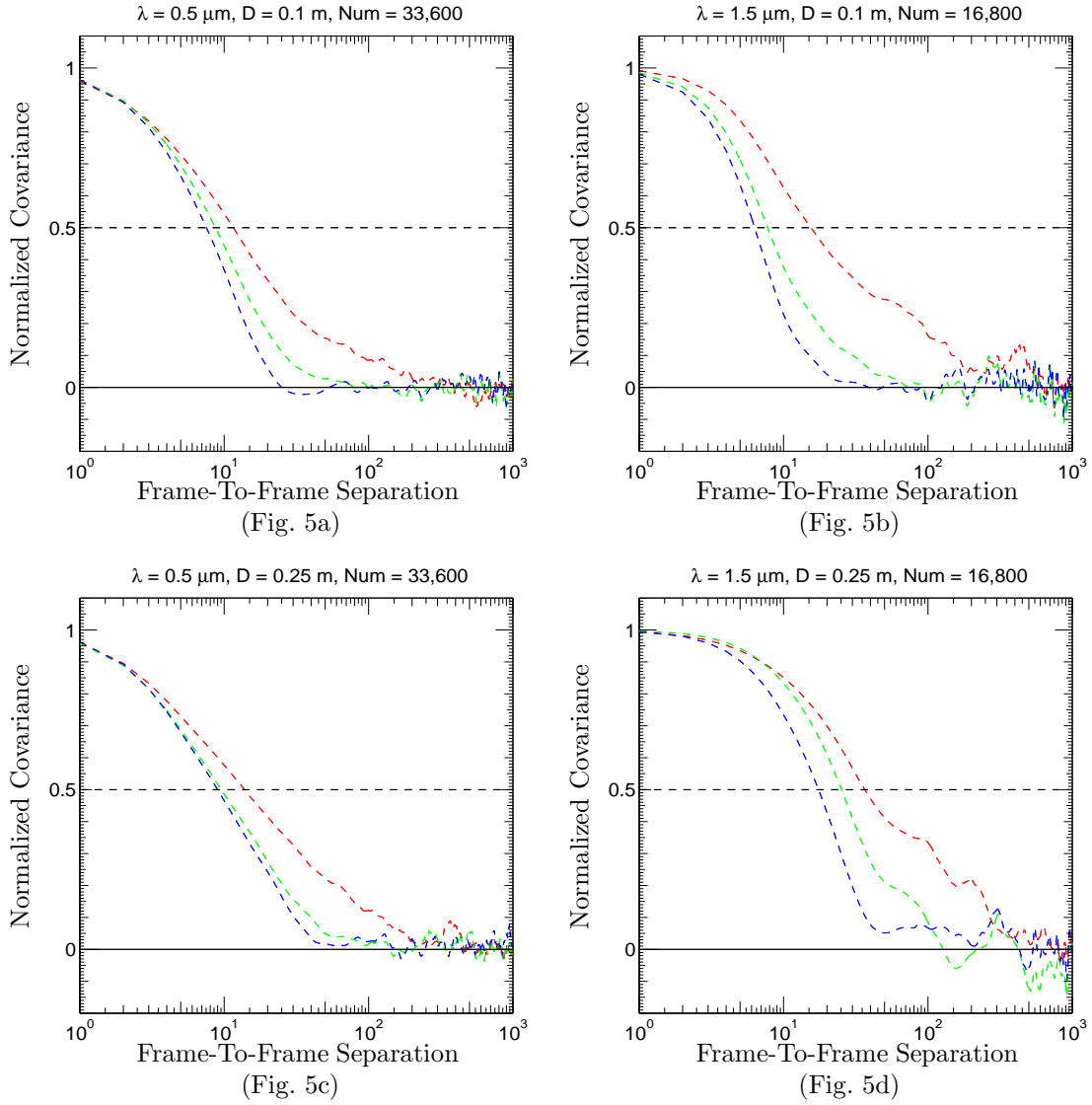


Figure 5. Normalized Correlation Of Successive Strehl Ratio Values

The three curves in each plot are to be associated with the similarly colored dashed line curves in the corresponding plots of Fig. 2 —the curves based on the wave optics propagation method. The normalized covariance is the covariance divided by the variance. The notation Num above each plot indicates the number of Strehl ratio values were used in producing the results shown in Fig. 2. The value of Num divided by the Frame-to-Frame Separation at which the normalized covariance curve crosses the 0.5 level can be taken as an estimate of the number of degrees-of-freedom in the data used forming the dashed line curves of Fig. 2.

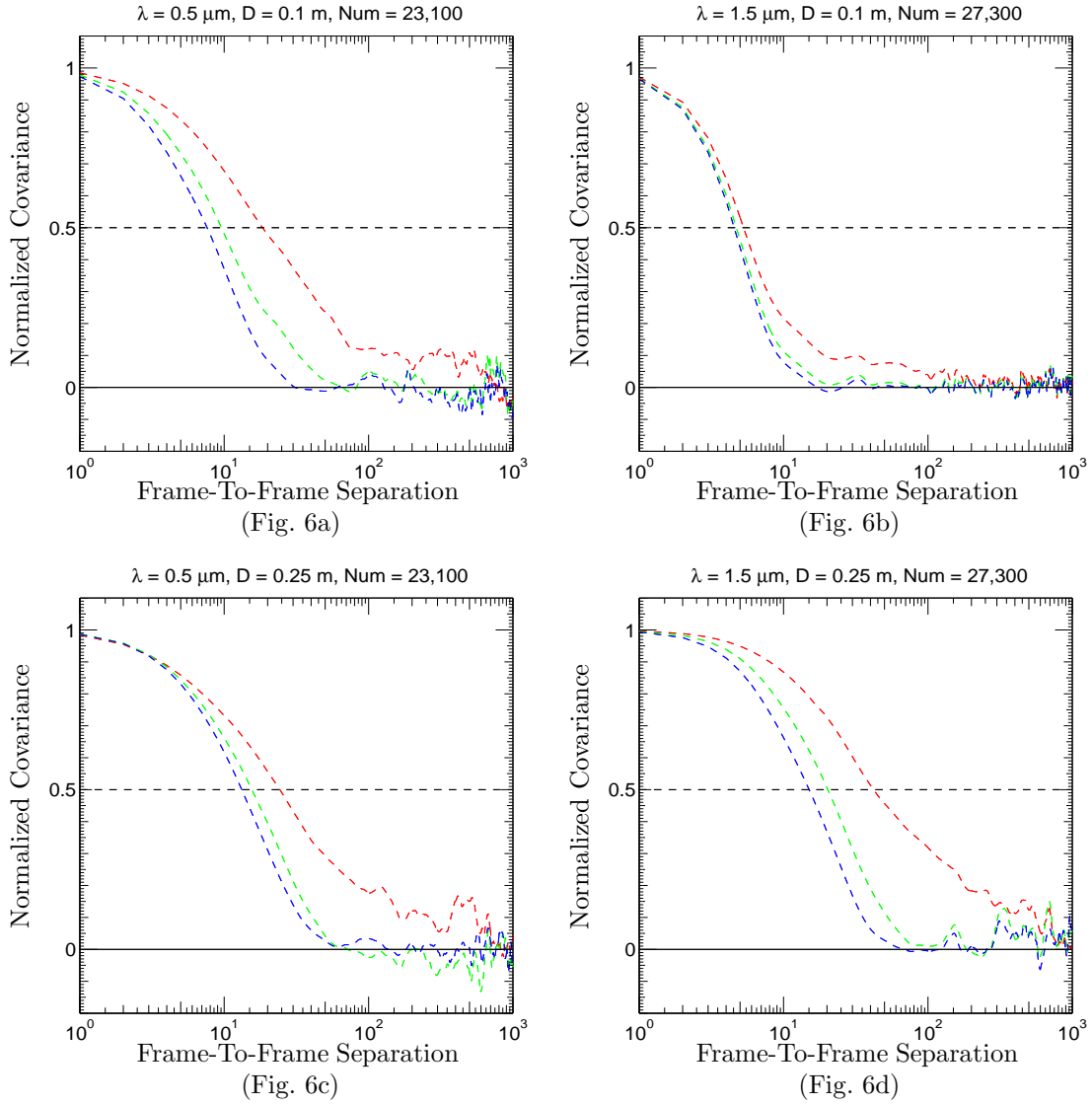


Figure 6. Normalized Correlation Of Successive Strehl Ratio Values

The three curves in each plot are to be associated with the similarly colored dashed line curves in the corresponding plots of Fig. 3 —the curves based on the wave optics propagation method. The normalized covariance is the covariance divided by the variance. The notation Num above each plot indicates the number of Strehl ratio values were used in producing the results shown in Fig. 3. The value of Num divided by the Frame-to-Frame Separation at which the normalized covariance curve crosses the 0.5 level can be taken as an estimate of the number of degrees-of-freedom in the data used forming the dashed line curves of Fig. 3.

Over all the agreement between the RytovProp results and the split-step wave optics propagation results shown in Fig.'s 1, 2, and 3 is quite good, especially when allowance is made for the smallness of the number of degrees-of-freedom of the data sets used to produce the wave optics propagation probability distribution curves (the dashed line curves). I take this as tending to validate the RytovProp method.

## 5. Acknowledgments

This work was performed under USAF/AFRL Contract No. FA9451-06-C-0348. I would like to thank Dr. Earl Spillar for his encouragement and support of this work. Also I wish to thank Dr. Michael Olier for a great deal of programming support (and for forcing me to pay attention to the occurrence of negative eigen-values and finding a way to formulate the analysis so that such eigen values do not show up.<sup>7</sup>). Lastly, I would like to thank Barry Foucault for making his wave optics propagation simulation results available to me.

---

<sup>7</sup> A covariance matrix can not have negative eigen-values